

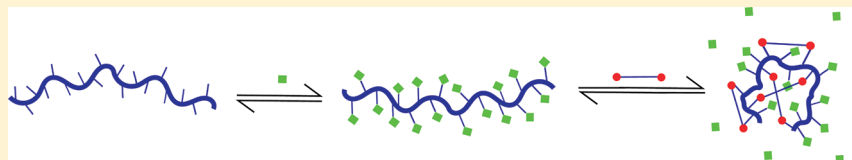
## Dynamic Covalent Single-Chain Polymer Nanoparticles

Benjamin S. Murray and David A. Fulton\*

Chemical Nanoscience Laboratory, School of Chemistry, Bedson Building, Newcastle University, Newcastle upon Tyne NE1 7RU, United Kingdom

Supporting Information

## ABSTRACT:



Polymeric nanoparticles were prepared through the chain collapse of linear polymers driven by the formation of dynamic covalent bonds. Linear chains of poly(vinylbenzaldehyde) were intramolecularly cross-linked through the formation of dynamic covalent acylhydrazone bonds with a bis-hydrazide cross-linker. The cross-linking density was shown to be controlled by the amount of cross-linker used. The resulting single polymer chain nanoparticles were then adorned through reaction of their remaining aldehyde units with a series of monoacyl hydrazides or alkoxyamines. Alternatively, the linear polymer chains could be fully adorned by reaction of their aldehyde units with the monoacyl hydrazides and then intramolecularly cross-linked through exchange reactions with the bis-hydrazide cross-linker. Both approaches proved effective routes to prepare single-chain polymer nanoparticles possessing high functional density.

Polymeric nanoparticles have found numerous applications in recent years in fields such as electronics,<sup>1</sup> coatings,<sup>2</sup> and drug delivery,<sup>3</sup> to name only a few. Intramolecular cross-linking of linear polymer chains has emerged<sup>4</sup> as a route to the preparation of structurally well-defined nanoparticles in the 5–20 nm range, which can be challenging to prepare using methods such as miniemulsion polymerization. A range of cross-linking chemistries have been employed to intramolecularly link linear polymer chains using clean and high yielding reactions. For example, the groups of Wooley and Hawker have utilized<sup>4i</sup> the reaction of amines with isocyanates to form ureas to cross-link isocyanate-containing copolymers by the addition of diamines. The ubiquitous Cu(I)-catalyzed cycloaddition of azides with alkynes has also been utilized<sup>4b</sup> to intramolecularly cross-link polymer chains possessing azido and alkyne groups, and the resulting nanoparticles can be further functionalized through reaction of azide functions within the nanoparticle with propargyl glycine utilizing the same chemistry. Covalent cross-linking approaches have also allowed access to collapsed polymers with a range of sizes and molecular architectures, such as diblock “tadpoles”,<sup>4d,h</sup> and globular nanoparticles capable of being adorned with various functionalities.<sup>4c,i</sup>

More recently, the incorporation of supramolecular cross-links into intramolecularly cross-linked polymer nanoparticles has introduced the virtue of reversibility, enabling a high degree of control in the chain collapse process. These reports have focused on self-complementary hydrogen-bonding functionalities to reversibly intramolecularly cross-link polymers under appropriate experimental conditions. Hawker et al. have utilized<sup>5</sup>

benzamide-containing dendrons to facilitate intramolecular cross-linking in toluene, while Meijer et al. have recently introduced<sup>6</sup> protected 2-ureidopyrimidone units coupled to urea or urethane moieties into polymer pendant arms and then induced single-chain collapse in  $\text{CHCl}_3$  in dilute conditions through 2-ureidopyrimidone deprotection by UV irradiation. Further impressive work by the group of Meijer describes a system where single-chain collapse in apolar solvent was achieved through UV deprotection of benzene-1,3,5-tricarboxamide (BTA) containing polymers, resulting in single-chain polymer nanoparticles with an internal helical architecture.<sup>7</sup> The BTA functionality was further incorporated into water-soluble copolymer systems where the helical folding of the polymer formed a hydrophobic compartment around a polymer-bound ruthenium catalyst, facilitating the transfer hydrogenation of substrates of limited aqueous solubility.<sup>8</sup>

We recently initiated a research program aimed at using ideas from the field of dynamic covalent chemistry (DCC)<sup>9</sup> to develop new polymer-based assemblies possessing responsive and adaptive properties. DCC uses reversible covalent bond formation to link component organic building blocks into larger structures, a process operating under thermodynamic control. The reversible nature of the dynamic covalent linkages enables polymer assemblies to modify their constitutions by incorporating or releasing components, in effect providing a mechanism for a polymer-based

Received: June 13, 2011

Revised: July 25, 2011

Published: September 02, 2011

assembly to reconfigure its covalent structure and therefore its functional or material properties.<sup>10</sup> The reversible nature of the linkages may also instill the “intelligent” virtues of controlled assembly, adaptability, and self-repair into the resultant polymer assemblies. Furthermore, the strength of the covalent bond ensures that product assemblies possess chemical robustness, and as reversible covalent reactions are usually performed with the help of a suitable catalyst to aid kinetics, the option exists to halt these reversible processes and kinetically “fix” the products simply by quenching the catalyst. We envisioned that by introducing dynamic covalent intramolecular cross-links into a linear polymer scaffold, we would be able to access sub-20 nm nanoparticles which possess the ability to undergo further structural reconfiguration in response to e.g. environmental changes or the addition of a suitable template. Subsequent decoration of these nanoparticles with organic residues, conjugated onto the cross-linked polymer through isoenergetic dynamic covalent bonds, would further enhance the potential of these particles to undergo structural reconfigurations. Indeed, the possibility exists that these structurally adaptable nanoparticles may be able to “mold” themselves around templates, reshuffling the cross-linkers or conjugated residues through exchange reactions as required to optimize binding between the two. Such an approach offers a potential mechanism to correct and refine binding sites, a virtue absent in molecularly imprinted polymers<sup>11</sup> where the molecular imprinting process is kinetically controlled, and there is no scope for error correction during the templating procedure. This deficiency leads to significant heterogeneity and binding pockets which are not optimized, with detrimental effects on molecular recognition.<sup>12</sup> The utilization of dynamic covalent bonds in such systems would also provide the necessary chemical robustness required to maintain the structural integrity of the nanoparticle, facilitating the application of these materials in environments that would be considered unsuitable for supramolecularly collapsed systems, e.g., acidic pH or high temperatures, while allowing controlled linkage exchange under defined experimental conditions to enable the material to adapt to applied stimuli.

In this work, we outline our first steps in the development of structurally adaptable single polymer nanoparticles. We describe the cross-linking of single polymer chains through dynamic covalent acylhydrazone bonds to prepare polymer nanoparticles, which can be further functionalized through adornment with small organic residues appended to the polymer chain also through dynamic covalent acylhydrazone linkages. We also demonstrate the structural reconfiguration of acylhydrazone-functionalized linear polymers into single polymer cross-linked nanoparticle architectures through exchange reactions.

## ■ EXPERIMENTAL SECTION

All chemicals and solvents were purchased from Sigma-Aldrich Co., Alfa Aesar, or Rathburn Chemicals Ltd. and were used as received without further purification. 4-Vinylbenzaldehyde (VBA) and poly(vinylbenzaldehyde) (PVBA) were prepared by the method described by Wooley et al.<sup>13</sup> 2,2'-((2-(*tert*-Butyl)-1,4-phenylene)bis(oxy))di-(acetohydrazide) (1),<sup>10a</sup> undecenoic acid hydrazide (2),<sup>10c</sup> *O*-(4-*tert*-butylbenzyl)hydroxylamine<sup>14</sup> (3), *O*-(2-hydroxyethyl)hydroxylamine (4),<sup>15</sup> and 2-(2-hydroxyethoxy)acetohydrazide<sup>16</sup> (5) were prepared according to their literature procedures. <sup>1</sup>H and <sup>13</sup>C NMR spectra were recorded on a Jeol ECS-400 spectrometer at 400 and 100 MHz or a Bruker Avance 300 spectrometer at 300 and 75 MHz, respectively, with the residual solvent signal as an internal standard. Gel permeation chromatography (GPC) was conducted in tetrahydrofuran on a Varian

ProStar instrument (Varian Inc.) equipped with a pair of PL gel 5  $\mu$ m Mixed D 300  $\times$  7.5 mm columns with guard column (Polymer Laboratories Inc.), a Varian 325 UV-vis dual wavelength detector (254 nm), a Dawn Heleos II multiangle laser light scattering detector (Wyatt Technology Corp.), and a Viscotek 3580 differential RI detector in series. Near-monodisperse polystyrene standards (Polymer Laboratories) were used for calibration. Data collection was performed with Galaxie software (Varian Inc.) and chromatograms analyzed with the Cirrus software (Varian Inc.) and Astra software (Wyatt Technology Corp.). Hydrodynamic diameters ( $D_h$ ) for polymers and nanoparticles in THF (1 mg mL<sup>-1</sup>) were determined by dynamic light scattering (DLS). The DLS instrumentation consisted of a MALVERN Instruments HPPS-ET 5002 operating at 25 °C with a 633 nm laser module. Measurements were made at a detection angle of 173° (backscattering), and Malvern DTS 4.20 software was utilized to analyze the data. The average of five measurements per sample is reported.

**Synthesis of P6.** 4-Vinylbenzaldehyde (0.335 g, 2.53 mmol), styrene (2.64 g, 25.3 mmol), *S*-1-dodecyl-*S'*-( $\alpha,\alpha$ -dimethyl- $\alpha''$ -acetic acid)trithiocarbonate (DDMAT) (18 mg, 0.049 mmol), and AIBN (1.7 mg, 0.01 mmol) were dissolved in 1,4-dioxane (3 mL), and the solution was degassed by three freeze-pump-thaw cycles. The yellow solution was then placed in oil at 70 °C for 17 h, and then the reaction was quenched by immersion in liquid N<sub>2</sub>. The reaction mixture was allowed to warm to room temperature and then precipitated by dropwise addition to MeOH (25 mL) to yield a coarse powder that was collected by filtration. The powder was then dissolved in 1,4-dioxane and precipitated by dropwise addition to MeOH (25 mL). The desired product was collected by filtration and then dried under high vacuum to yield a faint yellow powder (0.688 mg). The final polymer possessed a VBA:styrene monomer composition of 1:3.7—significantly different from the feed ratio of 1:10—reflecting the increased reactivity of VBA relative to styrene and suggesting the polymer obtained possessed a gradient distribution of monomers. <sup>1</sup>H NMR (CDCl<sub>3</sub>, 300 MHz):  $\delta$  9.89 (br, CHO), 6.56–7.53 (br, Ar), 3.25 (br, SCH<sub>2</sub>), 0.88–2.22 (br, polymer backbone and chain transfer agent protons). GPC (THF):  $M_n$  = 13 600,  $M_w$  = 17 250, PDI = 1.27.

**General Procedure for Synthesis of Cross-Linked Nanoparticles.** A solution of 2,2'-((2-(*tert*-butyl)-1,4-phenylene)bis(oxy))di-(acetohydrazide) in THF (half the volume of the PVBA solution) was added dropwise to a solution of PVBA in THF (1 mg mL<sup>-1</sup>) over 30 min. The colorless solution was allowed to stir at room temperature for a further 30 min, and then TFA was added dropwise (4 drops) and the solution left to stir for 12 h. The reaction mixture was quenched by the addition of NEt<sub>3</sub> and concentrated under reduced pressure to a volume of 2 mL; then the polymer was precipitated from solution by its dropwise addition to hexane (10 mL) and then isolated by filtration. The obtained powder was further washed with MeOH (2  $\times$  30 mL) and then dried under reduced pressure to leave the desired product as a powder possessing a faint yellow color. <sup>1</sup>H NMR (CDCl<sub>3</sub> + 5% CD<sub>3</sub>OD, 400 MHz):  $\delta$  9.80 (br, 1H, CHO), 6.52–7.45 (br, Ar and hydrazone protons), 4.70–5.12 (br, linker CH<sub>2</sub>), 3.04 (br, SCH<sub>2</sub>), 1.19–2.18 (br, polymer backbone, linker <sup>t</sup>Bu and chain transfer agent protons).

**General Procedure for Synthesis of Functionalized Cross-Linked Nanoparticles.** The required monohydrazide or alkoxyamine was added dropwise in THF (5 mL) to the crude nanoparticle solution obtained from the above procedure prior to quenching. The solution was left to stir for 12 h, quenched by the addition of NEt<sub>3</sub>, and concentrated under reduced pressure to a volume of 2 mL; then the polymer was precipitated from solution by its dropwise addition to hexane (10 mL) and then isolated by filtration. The obtained powder was further washed with MeOH (2  $\times$  30 mL) and then dried

under reduced pressure to leave the desired product as a faint yellow powder.

**NP1[20%]** Conjugate with **3** at 40% (**NP1[20%]-3[40%]**).  $^1\text{H}$  NMR ( $\text{CDCl}_3$ , 400 MHz):  $\delta$  9.81 (br, CHO), 6.48–8.00 (br, Ar, hydrazone and oxime protons), 4.70–5.12 (br, linker  $\text{CH}_2$  and residue  $\text{CH}_2$ ), 3.20 (br,  $\text{SCH}_2$ ), 0.87–2.36 (br, polymer backbone, linker  $^t\text{Bu}$ , residue  $^t\text{Bu}$  and chain transfer agent protons).

**NP2[20%]** Conjugate with **2** at 30% (**NP2[20%]-2[30%]**).  $^1\text{H}$  NMR ( $\text{CDCl}_3$  + 5%  $\text{CD}_3\text{OD}$ , 300 MHz):  $\delta$  9.73 (br, CHO), 5.87–8.42 (br, Ar and hydrazone protons), 5.73 (br, residue alkene  $\text{CH}$ ), 4.65–4.94 (br, alkene  $=\text{CH}_2$  and linker  $\text{CH}_2$ ), 3.15 (br,  $\text{SCH}_2$ ), 0.82–2.69 (br, polymer backbone, linker  $^t\text{Bu}$ , residue  $\text{CH}_2$  and chain transfer agent protons).

**NP2[20%]** Conjugate with **2** at 80% (**NP2[20%]-2[80%]**).  $^1\text{H}$  NMR ( $\text{CDCl}_3$  + 5%  $\text{CD}_3\text{OD}$ , 400 MHz):  $\delta$  5.86–8.69 (br, Ar and hydrazone protons), 5.74 (br, alkene  $\text{CH}$ ), 4.61–4.88 (br, alkene  $=\text{CH}_2$  and linker  $\text{CH}_2$ ), 3.13 (br,  $\text{SCH}_2$ ), 0.82–2.60 (br, polymer backbone, linker  $^t\text{Bu}$ , residue  $\text{CH}_2$  and chain transfer agent protons).

**NP2[20%]** Conjugate with **4** 60% (**NP2[20%]-4[60%]**).  $^1\text{H}$  NMR ( $\text{CDCl}_3$  + 5%  $\text{CD}_3\text{OD}$ , 400 MHz):  $\delta$  9.80 (br, CHO), 6.19–8.27 (br, Ar, hydrazone and oxime protons), 4.51–5.31 (br, linker  $\text{CH}_2$ ), 3.90–4.27 (br, residue  $\text{CH}_2$ ), 3.22 (br,  $\text{SCH}_2$ ), 0.83–2.54 (br, polymer backbone, linker  $^t\text{Bu}$  and chain transfer agent protons).

**General Procedure for Synthesis of Linear Conjugates of PVBA or P6 with Acylhydrazides/Alkoxyamines.** The required quantity (1 equiv) of monohydrazide or alkoxyamine in THF (half the volume of the polymer solution) was added dropwise to a solution of PVBA or **P6** in THF (1 mg  $\text{mL}^{-1}$ ) over 30 min. The colorless solution was allowed to stir at room temperature for a further 30 min, and then TFA was added dropwise (4 drops) and the solution left to stir for 12 h. The reaction solution was quenched by the addition of  $\text{NEt}_3$  and concentrated under reduced pressure to a volume of 2 mL; then the polymer was precipitated from solution by its dropwise addition to hexane (10 mL) and then isolated by filtration. The obtained powder was further washed with MeOH ( $2 \times 30$  mL) and then dried under reduced pressure to leave the desired product as a faint yellow powder.

**P1** Conjugate with **3** at 40% (**P1-3[40%]**).  $^1\text{H}$  NMR ( $\text{CDCl}_3$ , 400 MHz):  $\delta$  9.85 (br, CHO), 8.03 (br, oxime protons), 6.24–7.71 (br, Ar), 5.18 (br, residue  $\text{CH}_2$ ), 3.03 (br,  $\text{SCH}_2$ ), 0.87–2.28 (br, polymer backbone and residue  $^t\text{Bu}$  and chain transfer agent protons).

**P2** Conjugate with **2** at 100% (**P1-2[100%]**).  $^1\text{H}$  NMR ( $\text{CDCl}_3$ , 400 MHz):  $\delta$  8.22 (br, hydrazone protons), 5.86–7.39 (br, Ar), 5.73 (br, alkene  $\text{CH}$ ), 4.87 (br, alkene  $=\text{CH}_2$ ), 3.09 (br,  $\text{SCH}_2$ ), 0.80–3.09 (br, polymer backbone, residue  $\text{CH}_2$  and chain transfer agent protons).

**P2** Conjugate with **4** at 60% (**P2-3[60%]**).  $^1\text{H}$  NMR ( $\text{CDCl}_3$ , 400 MHz):  $\delta$  9.86 (br, CHO), 8.05 (br, oxime protons), 6.26–7.74 (br, Ar), 4.33 (br, residue  $\text{CH}_2$ ), 3.96 (br, residue  $\text{CH}_2$ ), 3.11 (br,  $\text{SCH}_2$ ), 1.19–2.32 (br, polymer backbone and chain transfer agent protons).

**P6** Conjugate with **2** at 100% (**P6-2[100%]**).  $^1\text{H}$  NMR ( $\text{CDCl}_3$ , 400 MHz):  $\delta$  6.35–7.72 (br, hydrazone and Ar protons), 5.79 (br, residue alkene  $\text{CH}$ ), 4.95 (br, residue alkene  $\text{CH}_2$ ), 3.25 (br,  $\text{SCH}_2$ ), 0.86–2.79 (br, polymer backbone, residue  $\text{CH}_2$  and chain transfer agent protons).

**P6** Conjugate with **5** at 100% (**P6-5[100%]**).  $^1\text{H}$  NMR ( $\text{CDCl}_3$ , 400 MHz):  $\delta$  6.26–8.09 (br, hydrazone and Ar protons), 4.58 (br, residue  $\text{OH}$ ), 4.15 (br, residue  $\text{CH}_2-\text{C}=\text{O}$ ), 3.64–3.76 (br, residue  $\text{CH}_2$ ), 0.81–2.22 (br, polymer backbone and chain transfer agent protons).

**Reduction of NP2[20%]-2[80%].** Sodium cyanoborohydride (24.5 mg, 0.39 mmol) was added as a solid to a solution of **NP2**-[20%]-2[80%] (12.1 mg,  $\sim 0.039$  mmol of hydrazone residues) in  $\text{CHCl}_3$ :MeOH (1 mL, 50:50). The suspension was stirred until it solubilized ( $\sim 5$  min) followed by the addition of TFA (1 drop). The solution was allowed to stir for 3 h; then solvent was removed under reduced pressure to leave a clear, colorless residue that was redissolved in

MeOH (2 mL) and then precipitated by the addition of  $\text{H}_2\text{O}$  (5 mL) with vigorous stirring. The solid was collected by centrifugation, resuspended in fresh  $\text{H}_2\text{O}$  (2 mL), and then isolated by centrifugation. This procedure was repeated twice followed by the drying of the collected solid under reduced pressure to leave the desired product as a white powder.  $^1\text{H}$  NMR ( $\text{CDCl}_3$ , 400 MHz):  $\delta$  5.91–7.21 (br, Ar), 5.78 (br, alkene  $\text{CH}$ ), 4.78–4.50 (m, alkene  $=\text{CH}_2$ ), 4.45–4.90 (br, linker  $\text{CH}_2$ ), 3.87 (br, benzyl protons), 0.87–2.60 (br, polymer backbone, linker  $^t\text{Bu}$ , residue  $\text{CH}_2$  and chain transfer agent protons).

**General Procedure for Dynamic Cross-Linking of Linear PVBA or P6 Conjugates.** To a solution of the linear polymer conjugate (0.1 mM) in THF was added bis-hydrazide linker **1** in THF (half the volume of the polymer solution) followed by a catalytic volume of TFA. The solution was left to stir and monitored periodically by GPC analysis. The reaction mixture was quenched when required by the addition of  $\text{NEt}_3$  and concentrated under reduced pressure to a volume of 2 mL; then the polymer was precipitated from solution by its dropwise addition to hexane (10 mL) and then isolated by filtration. The obtained powder was further washed with MeOH ( $2 \times 30$  mL) and then dried under reduced pressure to leave the desired product as a white powder.

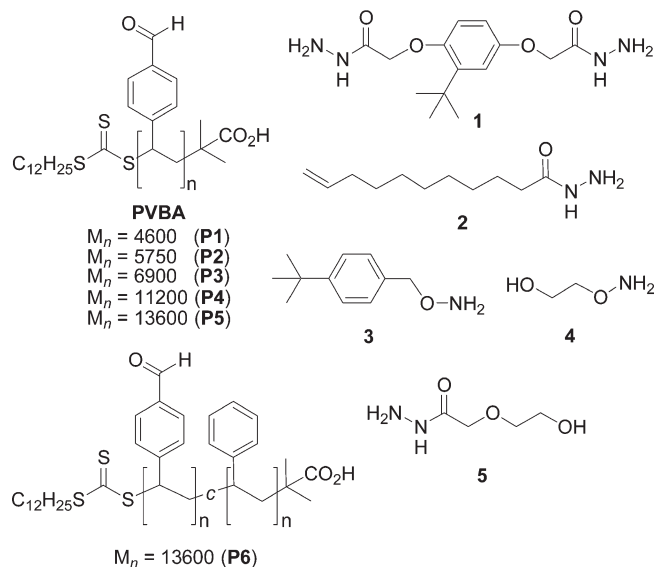
## RESULTS AND DISCUSSION

Poly(vinylbenzaldehyde) (PVBA) has been used previously<sup>10c</sup> by ourselves as a scaffold onto which acylhydrazide-containing functionalities may be efficiently grafted in high yield through acylhydrazone bond formation. Acylhydrazone exchange is a well-studied<sup>9</sup> reaction in the field of dynamic covalent chemistry and is catalyzed by acid, thus allowing the products to be kinetically fixed by neutralization. Macrocycles incorporating acylhydrazone bonds have been shown<sup>17</sup> to possess incredible abilities to reconfigure and optimize their structures to bind templates, demonstrating the considerable potential of this dynamic covalent reaction. The dynamic covalent acylhydrazone bonds thus may also endow single chain polymer nanoparticles with the abilities to reconfigure and optimize their structures. We envisaged that intramolecular collapse of a series of PVBA ( $M_n = 4.6$ –13.6 kDa) could be facilitated using the bis-hydrazide **1** as an intramolecular chain cross-linker. The polymer chain could then be functionalized further by reaction of its remaining aldehyde groups through acylhydrazone formation with organic residues, and for this model study the monoacylhydrazides or alkoxyamines **2**–**5** were chosen.

Initial cross-linking studies were performed utilizing the “parent” PVBA polymer scaffold **P2** ( $M_n = 5.75$  kDa). Dropwise addition of varying quantities of cross-linker **1** (5–30 mol % cross-linker **1** relative to the total number of aldehyde units within the polymer) to solutions of **P2** in THF followed by addition of a catalytic quantity of TFA was performed to yield a range of nanoparticles possessing varying densities of cross-links. The resulting reaction mixtures were typically left to stir for 12 h to allow intrapolymer conjugation to attain equilibrium, a process which results in complete reaction of all acylhydrazide groups and thus allows cross-linking density to be tuned by controlling the mol % of cross-linker added. The reactions were then kinetically fixed by quenching the TFA catalyst by the addition of  $\text{NEt}_3$ , followed by concentration of the polymer solution then precipitation into hexane. The precipitates were collected by filtration and then washed with MeOH to yield the cross-linked polymer chains as faint yellow powders. The quenching of trace amounts of TFA proved essential before concentration and subsequent isolation of polymer nanoparticles, as without this step inter-nanoparticle cross-linking and the



formation of insoluble films was observed, presumably as a consequence of acid-catalyzed acylhydrazone bond exchange between neighboring nanoparticles.<sup>10a</sup> It was observed that optimum polymer concentrations for conjugation reactions were  $\sim 0.1$  mM, as greater concentrations afforded nanoparticles possessing broader PDIs and higher molecular weights indicating the onset of interchain cross-linking.



It is worthwhile noting the nomenclature we have used through this work to describe our single polymer chain nanoparticles. Each linear polymer/copolymer (**P**) is assigned a number from 1 to 6 (see above structures and Table 1 for further information on each polymer). The resulting nanoparticle formed when the linear polymer is cross-linked is then given the prefix **N**. The percentage of aldehyde units within the polymer chain involved in cross-linking is given in square brackets. The further functionalization of a nanoparticle is indicated by an additional number from 2 to 5, which corresponds to the monohydrazides or alkoxyamines used (as shown above), and the degree of functionalization is given by a percentage in square brackets which indicates the percentage of aldehyde units which are functionalized. For example, **NP1**–[20%]–3[40%] indicates a cross-linked nanoparticle derived from **P1** where 20% of the available aldehyde units are involved in cross-linking and 40% of the aldehyde units have been functionalized with monoalkoxyamine 3.

Isolated nanoparticles were characterized by gel permeation chromatography (GPC). GPC proved to be a convenient method to monitor the volume changes from the collapse of a linear polymer<sup>4a–e,g–i,6,18</sup> into cross-linked nanoparticles, as this technique separates analytes based on their hydrodynamic volumes. In all cases, GPC analysis (Figure 1) revealed that the cross-linked polymers displayed highly symmetrical monomodal chromatograms possessing an increased retention time relative to the GPC trace of the “parent” polymer **P2**, indicating the collapse of the polymer chain and concomitant reduction in its hydrodynamic volume. These chromatograms also indicate the samples consist only of cross-linked single polymer chains. As the cross-linking density increased the retention time of the collapsed polymers also increased, up to a maximum of 30 mol % cross-linker **1**, where a slight reduction in retention time of

**Table 1.** Characterization of Polymers **P1**–**P6** and Collapsed Nanoparticles **NP1**–**NP6** Possessing Various Degrees of Cross-Linking, As Determined by Gel Permeation Chromatography (THF at 1 mL min<sup>−1</sup>) Calibrated against Near-Monodisperse Polystyrene Standards

	“parent” PVBA				nanoparticle			
	$M_n$	$M_w$	PDI		% linker	$M_n$	$M_w$	PDI
					hydrazide			
P1	4600	5550	1.21	NP1[20%]	20	3650	4400	1.21
P2	5750	6800	1.18	NP2[5%]	5	5650	6700	1.19
				NP2[10%]	10	5300	6300	1.19
				NP2[20%]	20	4550	5550	1.21
				NP2[30%]	30	4900	5850	1.19
P3	6900	8450	1.22	NP3[20%]	20	5900	7400	1.25
P4	11200	13300	1.19	NP4[20%]	20	8700	10 200	1.17
P5	13600	16000	1.17	NP5[20%]	20	9700	12 350	1.28
P6	13600	17250	1.27	NP6[50%]	50	10 700	13 850	1.29

**NP2**[30%] relative to **NP2**[20%] was found. This observation suggests that at higher cross-linking densities the polymer could collapse no further and the cross-linker itself was beginning to contribute significantly to the hydrodynamic volume of the collapsed particle.

<sup>1</sup>H NMR spectroscopy was used to further characterize the cross-linked nanoparticles, an example of which is presented in Figure 2 for the transformation of **P2** into **NP2**[20%]. The presence of diagnostic resonances at  $\delta = 4.7$ –5.1 ppm assigned to methylene protons within the cross-linking units confirmed their incorporation within the cross-linked nanoparticles, and integration of polymer aldehyde resonances against these methylene resonances confirmed that the degree of cross-linking reflected the feed quantity of the linker.

The cross-linked polymer nanoparticles were soluble in THF and DMSO, but in CH<sub>2</sub>Cl<sub>2</sub> or CHCl<sub>3</sub> required a small quantity of methanol to ensure complete dissolution. This observation could be attributed to multiple supramolecular H-bonding interactions between the acylhydrazone groups in neighboring nanoparticles. Indeed, the existence of interparticle H-bonding interactions have been reported by others in unimolecular cross-linked systems containing urea groups.<sup>4i</sup>

Cross-linking was then investigated with a series of “parent” PVBA of varying chain lengths (**P1**, **P3**–**P5**) (Table 1). In each case, cross-linking was performed with 20 mol % of cross-linker **1**, resulting in the formation of single polymer nanoparticles which were shown by GPC analysis (Figure 3 and Figure S1) to possess reduced hydrodynamic volumes relative to the “parent” linear polymers, as shown by the increased retention volume and concomitant decreases in “apparent”  $M_n$  of 15–30%. This analysis also showed that the PDIs of the cross-linked nanoparticles reflected those of the “parent” linear polymers (Table 1). Additionally, cross-linking experiments were performed on a copolymer derived from styrene and vinylbenzaldehyde (**P6**) which achieved a 50% aldehyde cross-linking density. Dynamic light scattering (DLS) analysis<sup>a</sup> (S2) of the “parent” polymers and their resultant cross-linked nanoparticle products indicated that the nanoparticle products are unimolecular, further evidence which excludes the presence of macromolecular dimers or higher-order cross-linked products.<sup>b</sup>

These cross-linked nanoparticles were further functionalized in a simple one-pot procedure by grafting monoacylhydrazides or

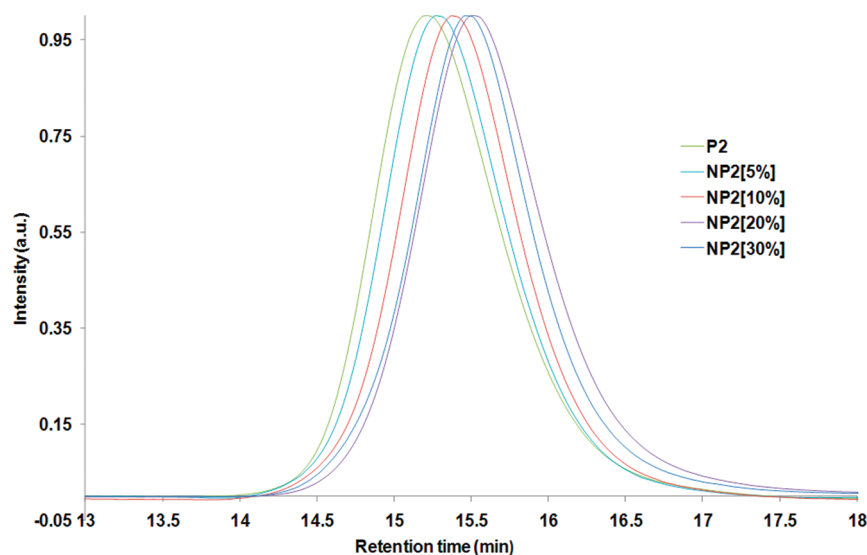


**Figure 1.** GPC RI traces of **P2** and collapsed nanoparticles **NP2**[5%–30%] obtained from the cross-linking of **P2** with varying amounts of bis-hydrazide cross-linker **1**.

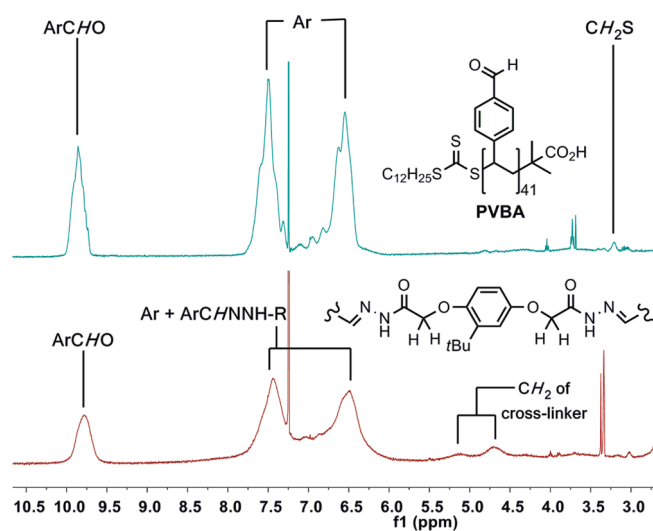


**Figure 2.**  $^1\text{H}$  NMR spectra (400 MHz) of **P2** ( $\text{CDCl}_3$ , top) and **NP2**[20%] ( $\text{CDCl}_3 + 5\% \text{CD}_3\text{OD}$ , bottom).

alkoxyamines (**2**–**5**) onto the nanoparticles through reaction with their remaining aldehyde units to create nanoparticles with among the highest density of functionality incorporated within their structure yet reported. After addition of the cross-linker **1** to the “parent” polymer solutions and subsequent nanoparticle formation was judged complete by GPC and  $^1\text{H}$  NMR spectroscopic analyses, a THF solution of the desired monoacylhydrazide or alkoxyamine was added dropwise. It was observed that the degree of functionality obtained in the isolated nanoparticle conjugates was controlled by and reflected the amount of monohydrazide or alkoxyamine added. Care was taken, however, not to introduce an excess of monohydrazide or alkoxyamine, relative to the number of free aldehyde units present within the nanoparticle, which could result in exchange and displacement of the cross-linkers which maintain the structural integrity of the nanoparticle. Again, GPC analysis facilitated monitoring of the progression of nanoparticle functionalization, and once completed,

the functionalized materials were isolated and purified as described for **NP1**–**NP6**.

Analysis of the GPC traces (Figure 4) of the functionalized nanoparticles **NP2**[20%]–**2**[30%] or [80%] revealed an increase in hydrodynamic volume relative to unfunctionalized **NP2**[20%] (and linear **P2**); however, this volume was still found to be less than that occupied by linear **P2** functionalized to the same extent with residue **2**. This data indicates that the cross-links remained intact during the functionalization procedure and the obtained products are functionalized unimolecular nanoparticles. This conclusion is further reinforced by analysis of the  $^1\text{H}$  NMR spectra of the functionalized products, confirming the conjugation of **2** onto the nanoparticle and, in the case of **NP2**[20%]–**2**[30%], also confirms the presence of the methylene protons associated the cross-linker (Figure 5). The  $^1\text{H}$  NMR spectrum (Figure 6a) of **NP2**[20%]–**2**[80%] was too broad to observe clearly the methylene protons associated with the cross-linker at  $\delta \sim 4.75$  ppm. This nanoparticle was kinetically fixed by reduction with  $\text{NaCNBH}_3$ , and the  $^1\text{H}$  NMR spectrum of the purified product was less broad and clearly confirmed (Figure 6b) the presence of cross-linker protons at  $\delta \sim 4.75$  ppm within the nanoparticle, in addition to the monohydrazide appendages.

Further functionalized nanoparticles were synthesized (Table 2), including **NP1**[20%]–**3**[40%], which is functionalized with **3** to a degree of 40%, and **NP2**[20%]–**4**[60%], which is functionalized with **4** to a degree of 60%. Using GPC analysis, these nanoparticles were then compared to their linear “parent” polymers which are adorned to the same extent with organic residues but possess no cross-links. The GPC trace (S3) of the functionalized “parent” polymer **P1**–**3**[40%] suggests a broader polymer distribution than that found in the cross-linked nanoparticle **NP1**[20%]–**3**[40%], indicating the cross-links confer control over the molecular architecture. Functionalization of the higher molecular weight **NP2**[20%] with **4** yielded a product of increased hydrodynamic volume but which was lower than that observed for its functionalized linear analogue (Figure 7). This observation again indicates the control that cross-linking

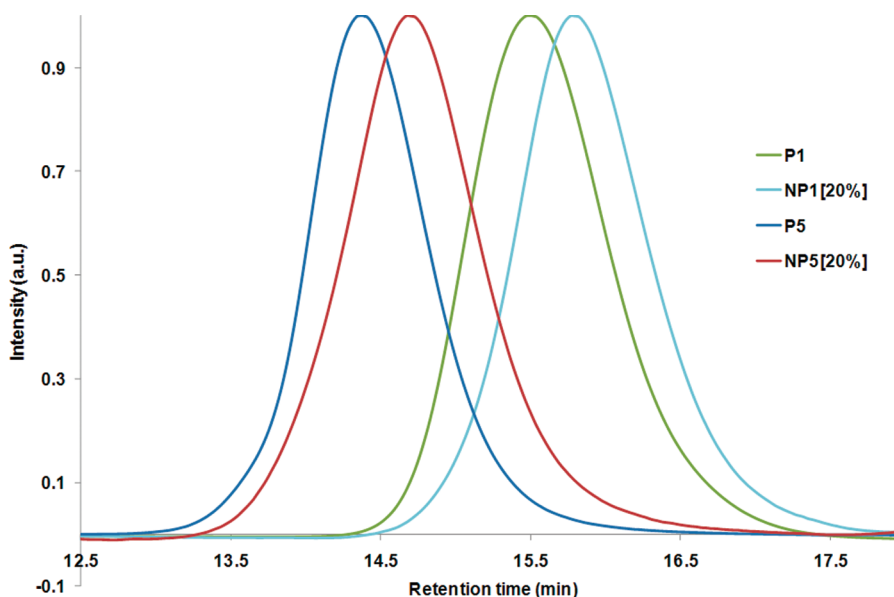


**Figure 3.** GPC RI traces of P1 and P5 and collapsed nanoparticles NP1[20%] and NP5[20%] obtained from the cross-linking of P1 and P5 with 20 mol% of cross-linker 1.

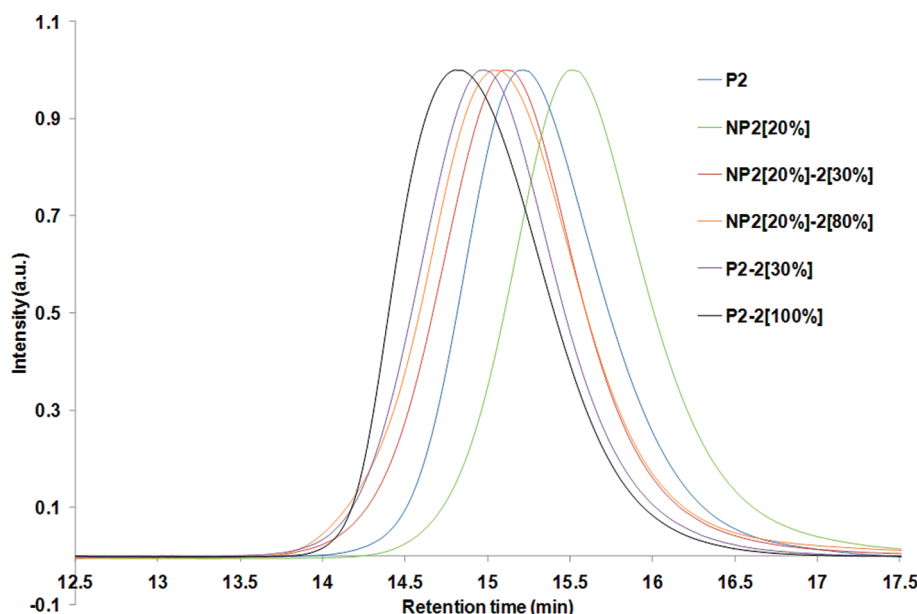


**Figure 4.** GPC RI traces of NP2[20%] functionalized with varying quantities of 2 and P2 also functionalized with vary quantities of 2.

confers over the architecture of the polymer nanoparticles.  $^1\text{H}$  NMR analysis of both nanoparticles (NP1[20%]-3[40%] and NP2[20%]-4[60%]) confirmed functionalization had occurred in each case and that linker methylene protons remained within the cross-linked product structures (Figure 8 and Figures S4 and S5).

Of great interest to us is the potential for structural adaptability that cross-linking through dynamic covalent acylhydrazone bonds may endow these functionalized nanoparticle systems. To begin to explore this possibility, we conducted some preliminary exchange experiments. A copolymer, P6 ( $M_n = 13.6$  kDa), was fully adorned with 2, and the resulting conjugate P6-2[100%] was characterized by  $^1\text{H}$  NMR spectroscopy to confirm the full

conjugation of the monohydrazide residues and the concomitant loss of the polymer aldehyde protons. Then, to a solution of P6-2[100%] in THF was added cross-linker 1 (50 mol %) under acid-catalyzed exchange conditions. GPC analysis was used to follow the change in polymer architecture as a function of time and revealed a decrease in hydrodynamic volume over 96 h (Figure 9). This volume reduction indicated that intrapolymer collapse through cross-linking had occurred via exchange of conjugated monohydrazide 2 with cross-linker 1. To further confirm acylhydrazone exchange had occurred, the polymeric material was analyzed by  $^1\text{H}$  NMR spectroscopy after isolation and purification (Figure 10), revealing the presence of the distinctive resonances associated with the methylene groups of 1, indicating its incorporation as a

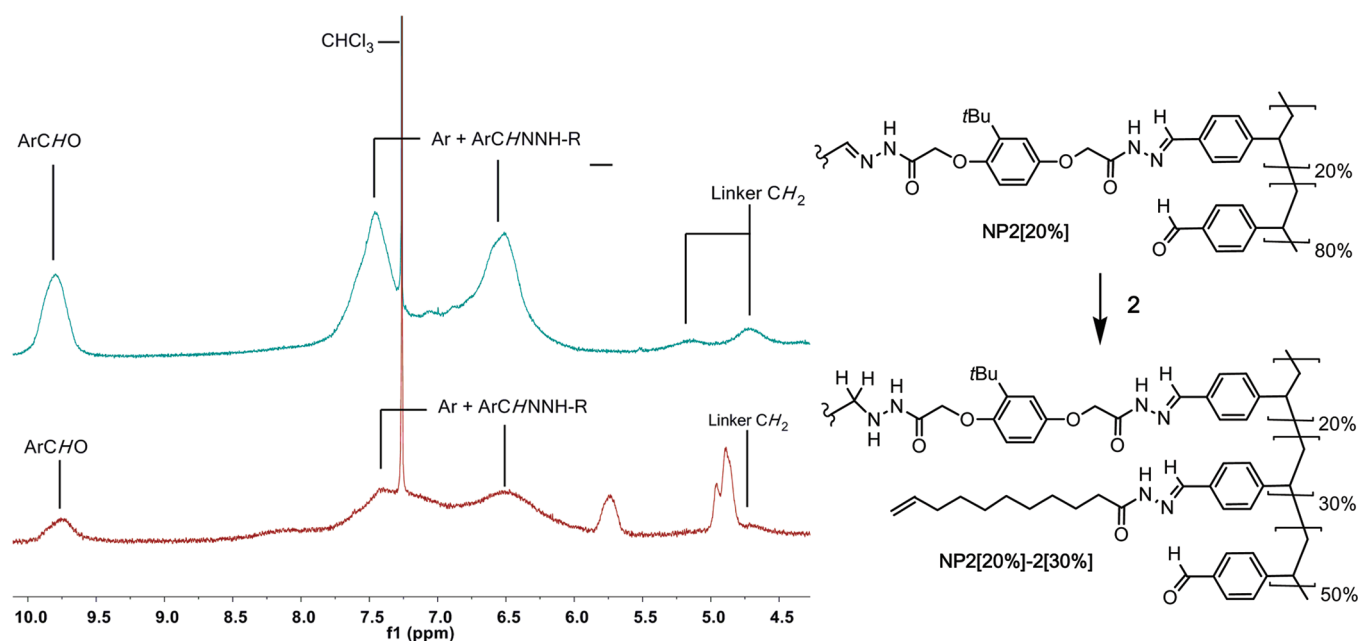


Figure 5. <sup>1</sup>H NMR spectra (CDCl<sub>3</sub> + 5% CD<sub>3</sub>OD) of NP2[20%] (400 MHz, top) and NP2[20%]-2[30%] (300 MHz, bottom).

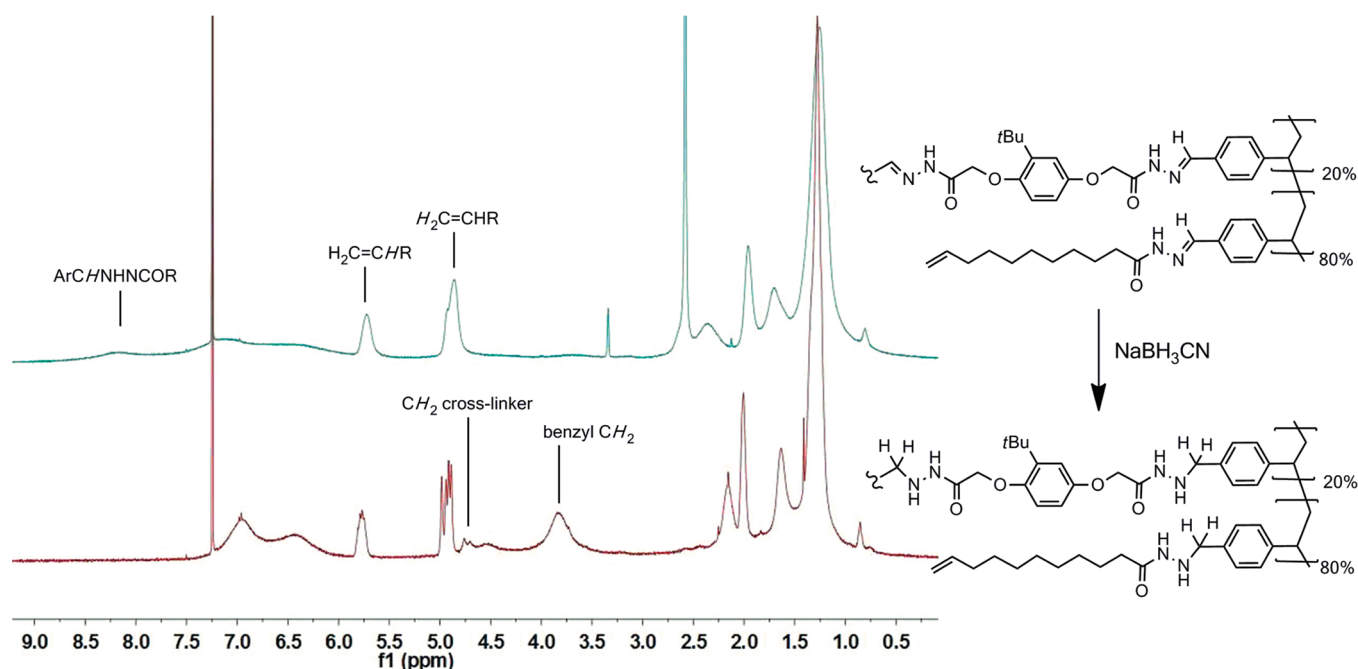


Figure 6. (a) <sup>1</sup>H NMR spectrum (400 MHz, CDCl<sub>3</sub> + 5% CD<sub>3</sub>OD) of NP2[20%]-2[80%] (top). (b) <sup>1</sup>H NMR spectrum (400 MHz, CDCl<sub>3</sub> after D<sub>2</sub>O shake) after hydrazone reduction and purification (bottom).

cross-linker into the polymer structure and further supporting the idea that hydrazone exchange had occurred.

The analogous exchange reaction was performed on a solution of **P2** fully adonred with monohydrazide **2** (**P2**–**2**[100%]), to which was added 20 mol % cross-linker **1**. GPC analysis (Figure 11) after 12 h indicated that intrapolymer cross-linking had occurred as evidenced by the presence of material of lower hydrodynamic volume relative to **P2**–**2**[100%], although some polymeric material of greater hydrodynamic volume was also observed, suggesting a minor amount of

interpolymer cross-linking. The volume distribution of polymeric material in solution stayed constant until 48 h, at which time the GPC trace displayed increased concentrations of material at lower elution volume, indicating the formation of material of greater hydrodynamic volume. Interestingly, the GPC traces obtained during the exchange reaction of **P2**–**2**[100%] with cross-linker **1** showed a broader distribution of material than the trace for NP2[20%]-2[80%], although both samples possessed material at the same lower hydrodynamic volume limit.

Table 2. GPC Data for Polymers P1–P2 and NP1–NP2 and Polymers and Nanoparticles Adorned with Organic Residues 2–4

	polymer				nanoparticle			
	$M_n$	$M_w$	PDI		% linker hydrazide	$M_n$	$M_w$	PDI
P1	4600	5550	1.21	NP1[20%]	20	3650	4400	1.21
P1–3[40%]	5400	6700	1.24	NP1[20%]-3[40%]	20	6250	7350	1.17
P2	5750	6800	1.18	NP2[20%]	20	4550	5550	1.21
P2–2[30%]	7700	9200	1.2	NP2[20%]-2[30%]	20	6650	8200	1.23
P2–2[100%]	8400	9800	1.17	NP2[20%]-2[80%]	20	6950	8650	1.24
P2–4[60%]	6850	8300	1.22	NP2[20%]-4[60%]	20	5550	7250	1.30

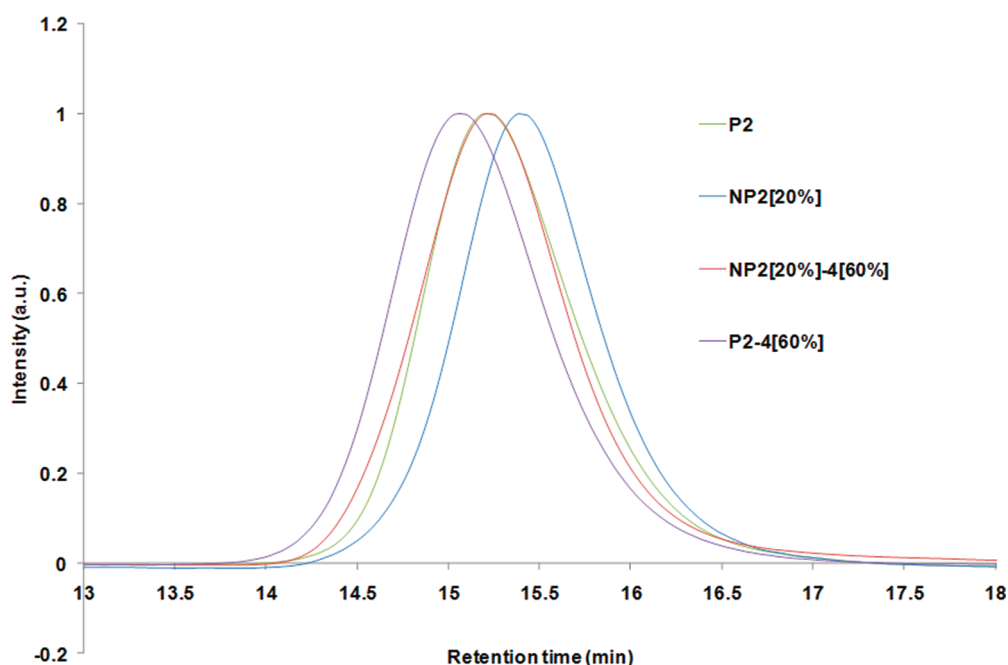
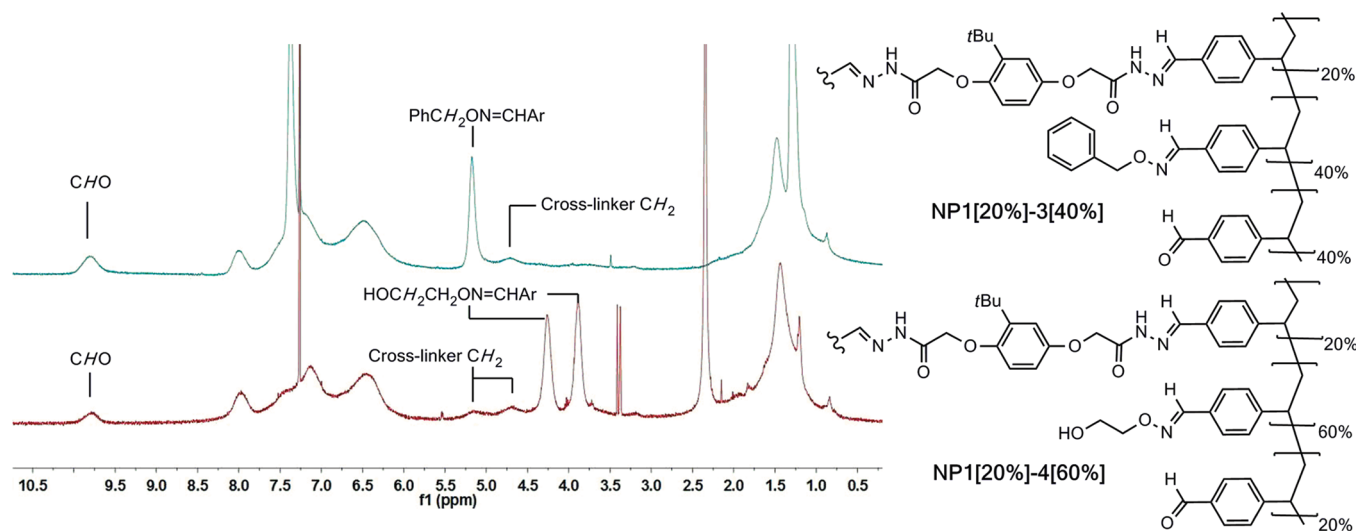
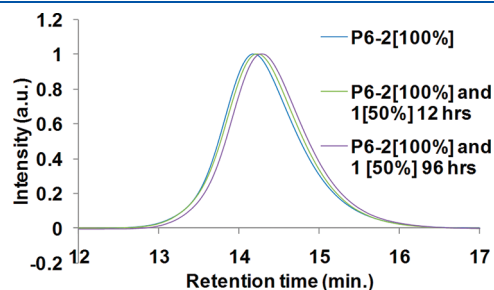


Figure 7. GPC RI traces for P2 and NP2[20%] before and after functionalization with residue 4.

Figure 8.  $^1\text{H}$  NMR spectrum (400 MHz,  $\text{CDCl}_3$ ) of NP1[20%]-3[40%] (top) and  $^1\text{H}$  NMR spectrum (400 MHz,  $\text{CDCl}_3 + 5\% \text{CD}_3\text{OD}$ ) of NP2[20%]-4[60%] (bottom).



A similar result was obtained through the collapse of **P6-5[100%]** through exchange with cross-linker **1**. GPC analysis (Figure 12) of the exchange reaction over 84 h revealed that



**Figure 9.** GPC RI traces for **P6-2[100%]** before and after cross-linking with cross-linker **1**.

after 12 h the polymer distribution spanned from collapsed material of lower hydrodynamic volume than **P6-5[100%]** to material of higher hydrodynamic volume than **P6-5[100%]**. This product distribution changed over the following 72 h, with the appearance of polymeric material with an apparent  $M_n$  10 times greater than the starting **P6-5[100%]**, and ultimately led to precipitation after 120 h. We observe that in both exchange experiments involving addition of **1** to **P6-5[100%]** or **P2-2[100%]** the kinetic product is that of the collapsed single polymer nanoparticles, and we hypothesize the collapsed polymer nanoparticles may then begin to aggregate in a process which is possibly induced by unfavorable interactions between the polymer and solvent. The aggregates themselves cross-link through hydrazone exchange between neighboring nanoparticles, resulting in the synthesis of polymeric material of greater hydrodynamic volume.

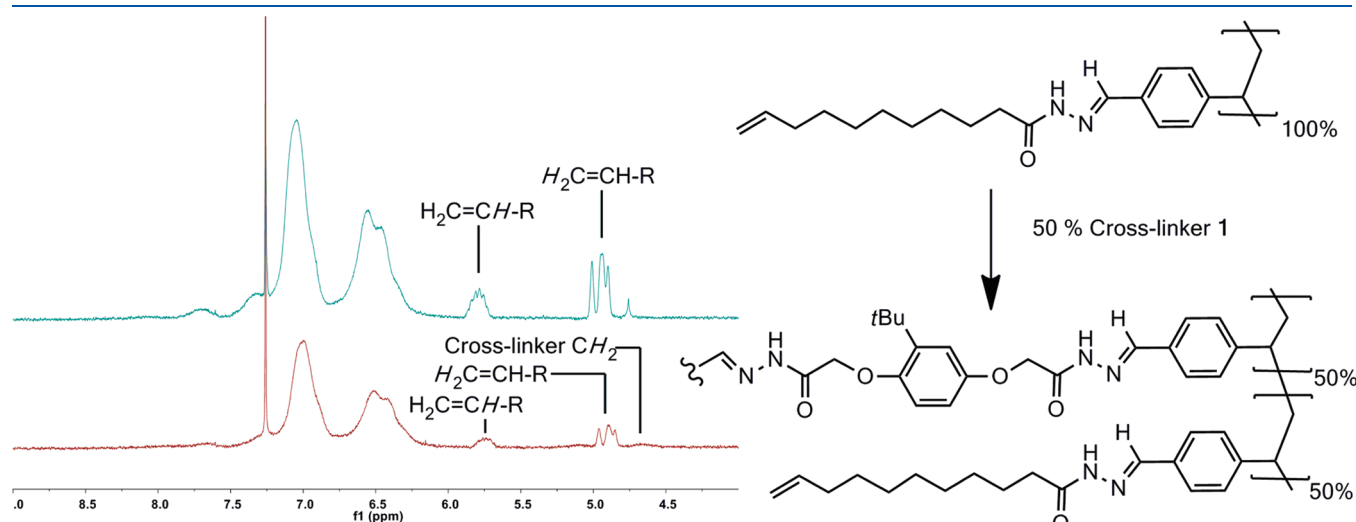


**Figure 10.**  $^1\text{H}$  NMR spectra (300 MHz,  $\text{CDCl}_3$ ) of **P6-2[100%]** (top) and the isolated nanoparticle after cross-linking (bottom).

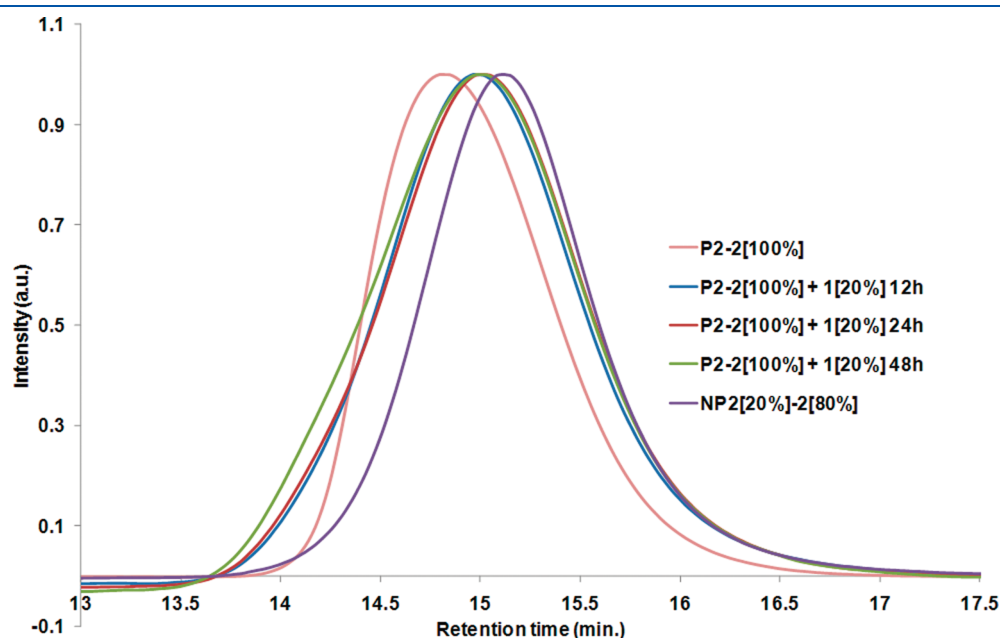


**Figure 11.** GPC RI traces following the collapse of the conjugated polymer **P2-2[100%]** after the addition of cross-linker **1** and of **NP2[20%]-2[80%]**.

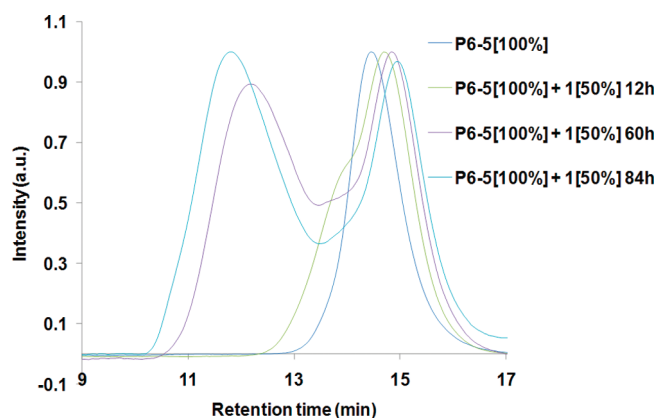


**Figure 12.** GPC RI trace following the collapse of the conjugated polymer P6–S[100%] after the addition of cross-linker 1.

## CONCLUSIONS

We have demonstrated that the intrapolymer collapse of linear PVBA (and a related copolymer) displaying aldehyde units can be driven by the formation of intramolecular dynamic covalent hydrazone bonds through reaction with a bis-hydrazide containing cross-linker, resulting in the formation of unimolecular nanoparticles whose architectural integrity is maintained and controlled. Further functionalization of the resulting nanoparticles was achieved by adorning the cross-linked nanoparticles with a range of low molecular weight organic hydrazides/alkoxyamines to obtain unimolecular nanoparticles with among the highest density of functionality incorporated within their structure yet reported. Furthermore, we were able to facilitate the collapse of linear PVBA (and copolymer P6) already fully adorned with organic residues through exchange reactions with a bis-hydrazide linker, demonstrating the ability to adapt the architecture of a single polymer chain through dynamic covalent chemistry. We are now focused on extending reversible intrapolymer cross-linking to water-soluble systems and extending the range of functionality incorporated into these nanoparticle systems. We believe this synthetic approach has great potential in the development of a new generation of polymeric materials whose structures are adaptable and may be “molded” around appropriate template molecules, or are responsive to external stimuli, and are investigating these possibilities.

## ASSOCIATED CONTENT

**Supporting Information.** Figures S1–S5. This material is available free of charge via the Internet at <http://pubs.acs.org>.

## AUTHOR INFORMATION

### Corresponding Author

\*E-mail: [d.a.fulton@ncl.ac.uk](mailto:d.a.fulton@ncl.ac.uk)

## ACKNOWLEDGMENT

We thank the EPSRC for generous support. The regional development agency One North East is also thanked for support.

## ADDITIONAL NOTE

<sup>a</sup> It was observed in all cases that upon cross-linking the apparent  $D_h$  of the parent polymers did not differ significantly from the obtained nanoparticles and was slightly larger for the NP than the parent polymer (<1 nm). A possible explanation for these observations may be that the presumably nonspherical architecture of the collapsed NPs may differ from that of the parent polymer such that its diffusion speed is reduced, thus increasing the calculated particle size. A further explanation may be that the collapse of linear polymers results in nanoparticle material that is relatively better solvated, particularly at the periphery of the particle, which contributes toward increasing its volume—again resulting in increased values of  $D_h$ . However, in light of GPC and NMR analysis providing firm evidence of cross-linking the DLS results at least indicate that the nanoparticle products are unimolecular, and the presence of macromolecular dimers or higher-order cross-linked products can be excluded.

<sup>b</sup> During the synthesis of collapsed polymer nanoparticles and their further functionalization we observed no cleavage of the trithiocarbamate functionality present in the polymer structures as a result of the use of the DDMAT chain transfer agent (CTA) during polymer synthesis, as determined by GPC and NMR analysis of the isolated nanoparticles where no higher-order aggregates were observed and resonances associated with the CTA were observed, respectively.

## REFERENCES

- (1) Landfester, K.; Antonietti, M. *Colloids Colloid Assem.* **2004**, 175–215.
- (2) Taylor, J. W.; Winnik, M. A. *J. Coat. Technol. Res.* **2004**, 1, 163–190.
- (3) (a) Oh, J. K.; Drumright, R.; Siegwart, D. J.; Matyjaszewski, K. *Prog. Polym. Sci.* **2008**, 33, 448–477. (b) Tyrrell, Z. L.; Shen, Y.; Radosz, M. *Prog. Polym. Sci.* **2010**, 35, 1128–1143.
- (4) (a) Mecerreyes, D.; Lee, V.; Hawker, C. J.; Hedrick, J. L.; Wursch, A.; Volksen, W.; Magbitang, T.; Huang, E.; Miller, R. D. *Adv. Mater.* **2001**, 13, 204–208. (b) Harth, E.; Van Horn, B.; Lee, V. Y.; Germack, D. S.; Gonzales, C. P.; Miller, R. D.; Hawker, C. J. *J. Am. Chem. Soc.* **2002**, 124, 8653–8660. (c) Jiang, J.; Thayumanavan, S. *Macromolecules* **2005**, 38, 5886–5891. (d) Pyun, J.; Tang, C.; Kowalewski, T.; Fréchet, J. M. J.; Hawker, C. J. *Macromolecules* **2005**, 38, 2674–2685. (e) Croce, T. A.; Hamilton, S. K.; Chen, M. L.; Muchalski, H.; Harth, E. *Macromolecules* **2007**, 40, 6028–6031. (f) Cherian, A. E.; Sun, F. C.; Sheiko, S. S.; Coates, G. W. *J. Am. Chem. Soc.* **2007**, 129, 11350–11351. (g) de Luzuriaga, A. R.; Ormategui, N.; Grande, H. J.; Odriozola, I.; Pomposo, J. A.; Loinaz, I. *Macromol. Rapid Commun.* **2008**, 29, 1156–1160. (h) Njikang, G.; Liu, G.; Curda, S. A. *Macromolecules* **2008**, 41, 5697–5702. (i) Beck, J. B.; Killops, K. L.; Kang, T.; Sivanandan, K.; Bayles, A.; Mackay, M. E.; Wooley, K. L.; Hawker, C. J. *Macromolecules* **2009**, 42, 5629–5635.
- (5) Seo, M.; Beck, J. B.; Paulusse, J. M. J.; Hawker, C. J.; Kim, S. Y. *Macromolecules* **2008**, 41, 6413–6418.
- (6) Foster, E. J.; Berda, E. B.; Meijer, E. W. *J. Am. Chem. Soc.* **2009**, 131, 6964–6966.
- (7) Mes, T.; van der Weegen, R.; Palmans, A. R. A.; Meijer, E. W. *Angew. Chem., Int. Ed.* **2011**, 50, 1–6.
- (8) Terashima, T.; Mes, T.; De Greef, T. F. A.; Gillissen, M. A. J.; Besenius, P.; Palmans, A. R. A.; Meijer, E. W. *J. Am. Chem. Soc.* **2011**, 133, 4742–4745.
- (9) (a) Rowan, S. J.; Cantrill, S. J.; Cousins, G. R. L.; Sanders, J. K. M.; Stoddart, J. F. *Angew. Chem., Int. Ed.* **2002**, 41, 898–952. (b) Corbett, P. T.; Leclaire, J.; Vial, L.; West, K. R.; Wietor, J.-L.; Sanders, J. K. M.; Otto, S. *Chem. Rev.* **2006**, 106, 3652–3711.

- (10) (a) Ono, T.; Fujii, S.; Nobori, T.; Lehn, J.-M. *Chem. Commun.* **2007**, 46–48. (b) Ura, Y.; Beierle, J. M.; Leman, L. J.; Orgel, L. E.; Ghadiri, M. R. *Science* **2009**, 325, 73–77. (c) Fulton, D. A. *Org. Lett.* **2008**, 10, 3291–3294. (d) Lehn, J.-M. *Prog. Polym. Sci.* **2005**, 30, 814–831. (e) Lehn, J.-M. *Chem. Soc. Rev.* **2007**, 36, 151–160.
- (11) Karlsson, B. C. G.; O'Mahony, J.; Karlsson, J. G.; Bengtsson, H.; Eriksson, L. A.; Nicholls, I. A. *J. Am. Chem. Soc.* **2009**, 131, 13297–13304.
- (b) Szabelski, P.; Kaczmarzski, K.; Cavazzini, A.; Chen, Y.-B.; Sellergren, B.; Guiochon, G. *J. Chromatogr., A* **2002**, 964, 99–111.
- (12) Zimmerman, S. C.; Lemcoff, N. G. *Chem. Commun.* **2004**, 5–14.
- (13) Sun, G.; Cheng, C.; Wooley, K. L. *Macromolecules* **2007**, 40, 793–795.
- (14) Mamalis, P.; Green, J.; Outred, D. J.; Rix, M. *J. Chem. Soc.* **1962**, 3915–3926.
- (15) Sebesta, D. P.; O'Rourke, S. S.; Martinez, R. L.; Pieken, W. A.; McGee, D. P. *C. Tetrahedron* **1996**, 52, 14385–14402.
- (16) Mahon, C. S.; Jackson, A. W.; Murray, B. S.; Fulton, D. A. *Chem. Commun.* **2011**, 47, 7209–7211.
- (17) (a) Furlan, R. L. E.; Ng, Y.-F.; Otto, S.; Sanders, J. K. M. *J. Am. Chem. Soc.* **2001**, 123, 8876–8877. (b) Roberts, S. L.; Furlan, R. L. E.; Otto, S.; Sanders, J. K. M. *Org. Biomol. Chem.* **2003**, 1, 1625–1633. (c) Furlan, R. L. E.; Cousins, G. R. L.; Sanders, J. K. M. *Chem. Commun.* **2000**, 1761–1762. (d) Cousins, G. R. L.; Furlan, R. L. E.; Ng, Y.-F.; Redman, J. E.; Sanders, J. K. M. *Angew. Chem., Int. Ed.* **2001**, 40, 423–428.
- (18) Schmidt, B. V. K. J.; Fechner, N.; Falkenhagen, J.; Lutz, J.-F. *Nature Chem.* **2010**, 3, 234–238.